

Comparative Structural Analysis and Kinetic Properties of Lactate Dehydrogenases from the Four Species of Human Malarial Parasites[†]

W. Michael Brown,[‡] Charles A. Yowell,[§] Anna Hoard,[‡] Thomas A. Vander Jagt,[‡] Lucy A. Hunsaker,[‡] Lorraine M. Deck,[⊥] Robert E. Royer,[‡] Robert C. Piper,^{||} John B. Dame,[§] Michael T. Makler,[#] and David L. Vander Jagt^{1,*}

Department of Biochemistry and Molecular Biology, University of New Mexico School of Medicine, Albuquerque, New Mexico 87131, Department of Chemistry, University of New Mexico, Albuquerque, New Mexico 87131, Department of Physiology and Biophysics, University of Iowa, Iowa City, Iowa 52242, Department of Pathobiology, College of Veterinary Science, University of Florida, Gainesville, Florida 32611, and FLOW Inc., Portland, Oregon 97201

Received January 14, 2004; Revised Manuscript Received March 19, 2004

ABSTRACT: Parasite lactate dehydrogenase (pLDH) is a potential drug target for new antimalarials owing to parasite dependence on glycolysis for ATP production. The pLDH from all four species of human malarial parasites were cloned, expressed, and analyzed for structural and kinetic properties that might be exploited for drug development. pLDH from *Plasmodium vivax*, *malariae*, and *ovale* exhibit 90–92% identity to pLDH from *Plasmodium falciparum*. Catalytic residues are identical. Residues I250 and T246, conserved in most LDH, are replaced by proline in all pLDH. The pLDH contain the same five-amino acid insert (DKEWN) in the substrate specificity loops. Within the cofactor site, pLDH from *P. falciparum* and *P. malariae* are identical, while pLDH from *P. vivax* and *P. ovale* have one substitution. Homology modeling of pLDH from *P. vivax*, *ovale*, and *malariae* with the crystal structure of pLDH from *P. falciparum* gave nearly identical structures. Nevertheless, the kinetic properties and sensitivities to inhibitors targeted to the cofactor binding site differ significantly. Michaelis constants for pyruvate and lactate differ 8–9-fold; Michaelis constants for NADH, NAD⁺, and the NAD⁺ analogue 3-acetylpyridine adenine dinucleotide differ up to 4-fold. Dissociation constants for the inhibitors differ up to 21-fold. Molecular docking studies of the binding of the inhibitors to the cofactor sites of all four pLDH predict similar orientations, with the docked ligands positioned at the nicotinamide end of the cofactor site. pH studies indicate that inhibitor binding is independent of pH in the pH 6–8 range, suggesting that differences in dissociation constants for a specific inhibitor are not due to altered active site pK values among the four pLDH.

The increasing incidence of *Plasmodium falciparum* malaria in many tropical and subtropical parts of the world reflects the spreading development of drug resistance of *P. falciparum* to most of the widely used antimalarials, including chloroquine, mefloquine, halofantrine, sulfadoxine, and pyrimethamine, and justifies referring to malaria as a reemerging disease (1). This makes it imperative to develop new antimalarial drugs whose targets differ from the targets of currently used drugs, due to the common problem of at least partial cross-resistance among drugs of similar structures. The number of antimalarials to which drug resistance is not widespread is small, reflecting the intense pressure on the available drug arsenal. Resistance is not yet widespread to the endoperoxides related to artemisinin; these will likely become major drugs of choice as resistance to the other

antimalarials spreads. It would be desirable to develop new antimalarials where the target is known and where the crystal structure of the target is available to aid in structure-based design of new drugs. In addition, it would be desirable to have new antimalarials that are effective against *Plasmodium vivax*, *Plasmodium ovale*, and *Plasmodium malariae* as well as *P. falciparum*, especially in view of emerging drug resistance patterns; for example, resistance of *P. vivax* to chloroquine is now developing rapidly (2).

During their erythrocytic cycles, malarial parasites depend extensively upon anaerobic glucose metabolism for ATP production and consequently exhibit levels of glucose consumption some 30–50-fold higher than their host cells (3, 4). For the most intensively studied human malarial parasite *P. falciparum*, the major product of glucose metabolism is L-lactate (3). The entire glycolytic pathway is present within this parasite, with many of the enzymes expressed at high levels compared to the erythrocyte (3, 5). Most of the glycolytic enzymes of *P. falciparum* have been cloned, including fructose biphosphate aldolase, glucose-6-phosphate isomerase, 3-phosphoglycerate kinase, hexokinase, glyceraldehydes-3-phosphate dehydrogenase, enolase, triose phosphate isomerase, and lactate dehydrogenase

[†] This work was supported by grant AI48239 from the National Institutes of Health.

* To whom correspondence should be addressed. Tel.: (505) 272-5788. Fax: (505) 272-3518. E-mail: dlvdnderjagt@salud.unm.edu.

[‡] University of New Mexico School of Medicine.

[§] University of Florida.

[⊥] University of New Mexico.

^{||} University of Iowa.

[#] FLOW Inc.

(pLDH)¹ (6–13). Due to the almost complete dependence that *P. falciparum* exhibits for ATP production from glucose metabolism, all of the enzymes of glycolysis represent potential drug targets. Several of these enzymes in *P. falciparum* have been analyzed by crystallography, including parasite pLDH (14), triosephosphate isomerase (15), and aldolase (16), which makes these enzymes especially attractive for structure-based drug design.

pLDH (EC 1.1.1.27) produces L-lactate from pyruvate while regenerating NAD⁺ for continued use in glycolysis. Thus, pLDH is essential for energy production in *P. falciparum* and was one of the first enzymes purified from *P. falciparum* (17). It was initially suggested that pLDH may be an attractive drug target on the basis of a number of unique kinetic properties that pLDH exhibits compared to LDH isoforms from human tissues (17). For example, mammalian LDH generally show substrate inhibition by pyruvate and are inhibited by the complex that forms between pyruvate and NAD⁺. It is generally agreed that pyruvate forms a very tight inhibitory complex with LDH and NAD⁺ in the steady-state reaction (18). pLDH, however, is weakly inhibited by pyruvate or the pyruvate–NAD⁺ complex, which suggests that the active site of pLDH has unique properties. Some of the unique kinetics of pLDH can be explained by the amino acid sequence of pLDH (13, 14). The important catalytic residues D168, H195, R171, and R109, which are essentially invariant in all LDH, are retained in pLDH. However, conserved residue Q102, which helps to define the active site of other LDH, on the basis of crystal data, is replaced by a lysine residue in pLDH; likewise, conserved residues T246 and I250, which help to define the cofactor binding site in most LDH, are both replaced by proline residues in pLDH. Moreover, in pLDH there is a unique five-amino-acid extension in the loop of amino acids that defines the substrate site (14). These differences make pLDH quite distinct from mammalian LDH and strongly suggest that pLDH should be an attractive target for development of selective inhibitors. In addition, known inhibitors of pLDH have been shown to exhibit antimalarial activities (19, 20).

Toxoplasma gondii is an obligate intracellular protozoan parasite responsible for toxoplasmosis, a disease that affects many mammals, including humans (21). *T. gondii* belongs to the phylum Apicomplexa, which includes a number of important pathogens besides *T. gondii*, including *Plasmodium* species. Numerous similarities between *T. gondii* and *P. falciparum* have been found at the biochemical level (22, 23). Several of the glycolytic enzymes from *T. gondii* and *P. falciparum*, including glucose-6-phosphate isomerase, enolase, and LDH, exhibit striking similarities between the two species (24–26). There are two forms of LDH in *T. gondii*, designated LDH1 and LDH2, which are differentially expressed in the proliferative tachyzoite and slowly dividing bradyzoite, respectively (26). LDH1 and LDH2 share 71% amino acid identity and are most similar to pLDH from *P. falciparum*, with 47% and 49% identity. Especially noteworthy is the presence of the five-amino-acid insert in the substrate specificity loop; this insert has only been observed

in pLDH and in LDH1 and LDH2 compared to all other LDH. The insert in LDH2 (DKEWS) is similar to the insert in pLDH (DKEWN) and differs slightly from the insert in LDH1 (DSEWS). Both LDH1 and LDH2 can utilize the NAD analogue 3-acetylpyridine adenine dinucleotide (APAD⁺) efficiently, similar to pLDH. The lack of strong substrate inhibition observed with pLDH is also observed with LDH2 (27). By comparison, LDH1 differs from LDH2 in exhibiting substrate inhibition, despite identical residues at the cofactor binding site that are thought to be critical for production of substrate inhibition (28).

The kinetic and sequence similarities among pLDH, LDH1, and LDH2 raise the question of whether LDH from Apicomplexa in general will exhibit similar properties and specifically whether pLDH from other *Plasmodium* species will show similar kinetic and structural properties compared to pLDH from *P. falciparum*. A related question is whether inhibitors targeted to pLDH from *P. falciparum* (29) will effectively inhibit all pLDH. In the present study, the pLDH from all four species of human malaria parasites were cloned and expressed, and the kinetic properties of the four pLDH were compared. In addition, homology structures of pLDH from *P. ovale*, *malariae*, and *vivax* were constructed from their protein sequences, and the crystal structure of pLDH from *P. falciparum*. The homology structures were used for molecular modeling studies to interpret the inhibitor binding properties of the four pLDH (designated pfLDH, poLDH, pvLDH, and pmLDH for *P. falciparum*, *ovale*, *vivax*, and *malariae*, respectively).

MATERIALS AND METHODS

Cloning of pvLDH, poLDH, and pmLDH. Genes encoding pLDH from *P. malariae* Uganda I (pmLDH), *P. ovale* Harding (poLDH), and *P. vivax* Salvador I (pvLDH) were obtained by PCR from genomic DNA prepared from blood-stage forms propagated in nonhuman primates. The parasitized blood was kindly provided by Dr. William E. Collins, CDC, Atlanta. Gene segments encoding 313 amino acids of pmLDH and poLDH were obtained using PCR primers (JNB 272 and JNB 273) designed from conserved 5′ and 3′ regions of the gene identified from alignments of the pLDH gene sequences of *P. falciparum*, *P. berghei*, and *P. yoelii* identified initially among unannotated genome sequence data (current PlasmoDB 4.1 identifiers Pf13_0141, Pb_232c03qlc, and chrPyl_01158, respectively). The pvLDH gene was obtained in two steps using primers JNB 284 and JNB 278 to obtain the 3′ half of the gene and identify an appropriate 3′ primer. This was followed by obtaining the remainder of the gene using primer JNB 309 designed at the 5′ end, based upon the *P. knowlesi* pLDH sequence (Sanger PKN.0.006043) identified in the unannotated genome sequence data and JNB 278. The PCR-amplified gene segments were each cloned in the plasmid Topo 2.1 and sequenced (GenBank accession numbers for poLDH, AY486058; pmLDH, AY486059; pvLDH, AY486060). In all cases, the gene segments encode 313 amino acids extending from the 5′ start to within approximately two amino acids of the natural 3′ end, with regions between the conserved primers representing the exact sequences of the pLDH from these species. The sequences derived from the conserved primers from poLDH and pmLDH must be viewed as only approximate since these have not been independently obtained. Alignment of the

¹ Abbreviations: LDH, lactate dehydrogenase; pLDH, parasite lactate dehydrogenase; pfLDH, poLDH, pvLDH, and pmLDH, lactate dehydrogenases from *Plasmodium falciparum*, *ovale*, *vivax*, and *malariae*, respectively; APAD⁺, 3-acetylpyridine adenine dinucleotide.

pvLDH sequence with that which has subsequently become available in the TIGR database (Pv_402775) indicates the following differences. The second amino acid is Ala instead of Thr, and the 310th amino acid is Arg rather than Lys. The gene segment expressed is missing the codons for the ultimate and penultimate amino acids, Ala and Leu, which are also predicted to be absent in the gene segments cloned to express pmLDH and poLDH.

Primer sequences

JNB 272	ATGGCACCAAAAGCAAAAAT
JNB 273	GCCTTCATTCTSYTAGTTTCAGC
JNB 278	GCCTTCATTCTSYTBGTYTCBGC
JNB 284	GCNCATGGNAAYAARATGGT
JNB 309	ATGGCNCNAARCCNAARAT

Expression and Purification of pLDH. The four pLDH were expressed in *Escherichia coli* as described previously for pfLDH (29). Antipain, leupeptin, imidazole, lactic acid, pyruvate, NAD, NADH, and EDTA were obtained from Sigma. Blue Sepharose CL-6B, PD-10 desalting column, chromatofocusing resin PBE 94, and chromatofocusing polybuffer 74 were from Pharmacia Biotech. Amicon YM-10 pressure filtration membranes were from Millipore. The purification of pLDH from lysate obtained by disruption of *E. coli* containing recombinant pLDH was carried out utilizing a rapid and efficient purification scheme. Routinely, approximately 100 mL of lysate was diluted into 200 mL of cold 10 mM Tris-HCl buffer, pH 8, containing 0.25 mM EDTA. A cocktail of protease inhibitors (antipain, bestatin, chymostatin, pepstatin A, and leupeptin) was added to a final concentration of 1 μ g/mL. This solution was loaded onto a Blue Sepharose CL-6B column (65 \times 130 mm) equilibrated with 40 mM Tris-HCl buffer, pH 8, containing 1 mM EDTA. The column was then washed thoroughly (two bed volumes or 500 mL) with 40 mM Tris-HCl buffer, pH 8, containing 1 mM EDTA. Finally, the pLDH was eluted from the column with 40 mM Tris-HCl buffer, pH 8, containing 1 mM EDTA, 0.15 M NaCl, and 7.5 mM NAD. The eluent was concentrated to 7.5 mL by pressure filtration in an Amicon apparatus fitted with a YM-10 membrane. The concentrated pLDH was desalted on a PD-10 column and was immediately loaded onto the chromatofocusing column (8 mm \times 155 mm) of PBE 94 resin, equilibrated with 25 mM imidazole buffer, pH 7.4. The chromatofocusing column was developed with 54 mL of polybuffer 74 (1:8 dilution with Millipore filtered water) at pH 4, containing 1 mM NAD. Active fractions were pooled. The pLDH sample was almost homogeneous (>95%) at this point, as shown by SDS-PAGE (20% with 5% stacking gel) with silver staining.

The final step in purification was carried out utilizing a Bio-Gel hydroxylapatite column (Bio-Rad Econo-Pac CHT-II cartridge). Material from the chromatofocusing step was again desalted as above and concentrated to 0.5 mL volume using Amicon Centricon filter devices (YM-30 molecular weight membrane by Millipore). The material was injected directly on the HPLC column and developed with a 45 min linear phosphate gradient from 10 mM sodium phosphate buffer, pH 6.8, containing 100 mM NaCl and 0.01 mM calcium chloride to 350 mM sodium phosphate buffer, pH

6.8, containing 100 mM NaCl and 0.01 mM calcium chloride with a flow rate of 0.5 mL/min. One-milliliter fractions were collected, and active fractions were frozen.

Kinetic Studies. LDH activity in the direction of reduction of pyruvate to L-lactate was measured in 1 mL of 0.1 M sodium phosphate buffer, pH 7.5, containing 10 mM pyruvate and 0.1 mM NADH at 340 nm. Activity measured in the direction of oxidation of L-lactate to pyruvate was assayed in 1 mL of 0.1 M Tris-HCl buffer, pH 9.2, containing 0.2% Triton X-100, 100 mM lactate, and 1 mM NAD⁺ at 340 nm ($\epsilon = 6.2 \text{ mM}^{-1} \text{ cm}^{-1}$). Michaelis constants for substrates and cofactors and k_{cat} values were determined from initial rate measurements at 25 $^{\circ}\text{C}$ by nonlinear regression analysis with the ENZFITTER program (Elsevier-Biosoft). Dissociation constants of inhibitors were determined from double-reciprocal plots by linear regression analysis. Inhibitors were prepared in stock solutions of DMSO. Concentrations of DMSO during the initial rate measurements did not exceed 0.5%. The synthesis of the inhibitors was described previously (19, 20).

Homology Modeling. Homology models were generated using the software Modeler (30). The structure of pfLDH (PDB code 1LDG) was used as a template. The sequence alignment used for generation of the probability density function is presented herein. For each species, 100 models were generated on the basis of starting structures with random backbone deviations from the template structure. The refinement (MD_LEVEL) was set to one, the deviation was set to 4.0, and the software was instructed to generate an all-atom hydrogen model for each species. The lowest energy structure from each was isolated for further refinement. The selected structures were superimposed onto the structure of pfLDH using the McLachlan algorithm (31) as implemented in ProFit 2.2. The ligand atoms (NADH and oxamic acid) were incorporated into each structure using the conformations and positions in 1LDG under the fitted frame of reference. The structures were examined to verify that no steric overlap existed between ligand and protein atoms. The refinement for all structures was then performed using the CVFF force field within the Discover software package (Accelrys Inc., San Diego, CA, 2000). All structures were soaked in four layers of explicit solvent and refined using a room-temperature relaxation protocol consisting of several stages of molecular dynamics along with steepest descents and conjugate gradient minimizations. Briefly, the initial stages of the relaxation consisted of steepest descents minimization, followed by conjugate gradient minimization, followed by minimal room temperature dynamics for only the added solvent molecules. This was followed by pairs of steepest descents and conjugate gradient minimization using a backbone tethering restraint that was reduced from 1000 kcal/ \AA^2 to 0 over four steps. The final derivative criteria for the last conjugate gradient minimization was 0.10 kcal/ \AA^2 . In all cases, the ligand atoms were held rigid. The resulting structures for all four species were analyzed using ProCheck to ensure stereochemical quality (32).

Inhibitor Docking. Inhibitor docking studies were performed with AutoDock 3.0 (33), which performs flexible ligand docking to a rigid target utilizing precalculated grids for energy evaluations. For the docking studies, the inhibitor partial charges were calculated on the basis of Gasteiger-Huckel rules as implemented in Sybyl (Tripos Inc., St. Louis,

MO, 2001). Geometry optimization of the inhibitor was performed using the BFGS algorithm. For each pLDH structure, Kollman all-atom partial charges were used to maintain consistency with the AutoDock free energy equation. (Note: Although an all-atom model was used for electrostatic calculations, nonpolar hydrogens were ignored for van der Waals calculations that utilized united-atom Lennard-Jones potentials.) The energetic grids were centered on the pLDH crystallographic ligands center of mass and dimensioned as a 22.5 Å cubic grid (0.375 grid point spacing). The dockings were performed using the Lamarckian genetic algorithm with a population size of 50, 1.5×10^6 energy evaluations, a mutation rate of 0.2, a crossover rate of 0.8, and a local search frequency of 0.06. For each species, 100 runs were performed.

RESULTS

Purification of pLDH. Each pLDH was expressed in *E. coli*; after cell lysis, the crude material was purified by extraction of all pLDH onto a Blue Sepharose affinity matrix, followed by further purification by chromatofocusing and hydroxylapatite chromatography. Purified pLDH, pmLDH, pvLDH, and poLDH showed specific activities 253, 216, 450, and 215 $\mu\text{mol min}^{-1} \text{mg}^{-1}$, respectively, for the reduction of pyruvate by NADH, pH 7.5, and showed apparent isoelectric points 6.5, 8.4, 6.2, and 8.0, respectively.

Sequence Comparisons of pLDH. All four pLDH retain the catalytic residues R109, D168, R171, and H195 that are essentially invariant to all LDH (Figure 1). A number of other highly conserved LDH residues, including G27, G29, G32, D65, A98, N116, N140, P141, D143, S153, G154, G162, L167, and E311, are also conserved in all pLDH. There are a total of 17 highly conserved LDH residues that are not conserved in pLDH (Figure 1). This includes Q102, a residue involved in pyruvate binding in LDH, which is K102 in all pLDH, and T246 and I250, conserved residues involved in cofactor and substrate binding, which are P246 and P250 in all pLDH. These changes are especially significant for drug development because they are active-site residues. Generally, the 17 changes in pLDH compared to other LDH lead to identical residue changes in all pLDH. There are exceptions, however; for example, highly conserved L110 in other LDH is retained in pLDH but is an aspartate residue in the other pLDH. Likewise, conserved residue K243 is a histidine in pLDH, poLDH, and pmLDH but a leucine in pvLDH. There are 50 sites where there are differences among the residues in the four pLDH. The most prominent difference between pLDH and other LDH is the expanded substrate specificity loop. All pLDH contain the same five-amino-acid insert (DKEWN) immediately in front of the conserved catalytic residue R109.

Substrate and Cofactor Properties of pLDH. The four pLDH were compared for their substrate properties with pyruvate and lactate, at pH 7.5 and 9.2, respectively (Table 1). For pyruvate, Michaelis constants varied 5-fold and k_{cat} values varied 2-fold, leading to catalytic efficiencies, k_{cat}/K_m , of 4.4×10^7 – $2.4 \times 10^8 \text{ M}^{-1} \text{ min}^{-1}$, similar to the catalytic efficiencies of human LDH (34). For lactate, Michaelis constants varied 9-fold and k_{cat} values varied 3-fold.

The four pLDH were also compared for their cofactor properties with NADH, NAD^+ , and the NAD^+ analogue

hLDHA	ATLKDQLIYNLLKEEQTPQNKITVVGVGAVGMACAIISILMKDLADELALV
pLDH	APKAKIVLVGSGMIGGVMATLIVQKNLGD VVLF
poLDH	MAPKAKIVLVGSGMIGGVMATLIVQKNLGD VVMF
pmLDH	MAPKAKIVLVGSGMIGGVMATLIVQKNLGD VVMF
pvLDH	MAPKAKIVLVGSGMIGGVMATLIVQKNLGD VVMF
102	
hLDHA	DVIDEKLKGEEMDLQHGSLFL RTPKIVSGKDYNTANSKLVIITAGARQ
pLDH	DIVKNMPLGKALDTSHTNVMAYSNCQVSGSNTYDDLAGSDVIVTAGFTK
poLDH	DIVKNMPLGKALDTSHTNVMAYSNCQVSGSNTYEDLKGADVIVTAGFTK
pmLDH	DIVKNMPLGKALDTSHTNVMAYSNCQVSGSNTYEDLKGADVIVTAGFTK
pvLDH	DIVKNMPLGKALDTSHTNVMAYSNCQVSGSNTYEDLKGADVIVTAGFTK
109	
hLDHA	QEGES RLNLVQRNVNIFKFIIIPNVKYSNCKLLIVSNPVDILTY
pLDH	APGKSDKEWNRLDLLPLNNKIMIEIGGHKNCNPAFIIVVTNPFVDMVQ
poLDH	APGKSDKEWNRLDLLPLNNKIMIEIGGHKNCNPAFIIVVTNPFVDMVQ
pmLDH	APGKSDKEWNRLDLLPLNNKIMIEIGGHKNCNPAFIIVVTNPFVDMVQ
pvLDH	APGKSDKEWNRLDLLPLNNKIMIEIGGHKNCNPAFIIVVTNPFVDMVQ
163 168 171 195	
hLDHA	VAWKISGFPKRVISGSGNLSARFRLMGERLGVHPLSCHGWVLEHGD
pLDH	LLHQHSGVPKNIIGLGGVLDTSRLKYYISQKLVNCPRDVNAHIVGAHGN
poLDH	LLHQHSGVSKNKIVGLGGVLDTSRLKYYISQKLVNCPRDVNAHIVGAHGN
pmLDH	LLHKHSGVPKNIIGLGGVLDTSRLKYYISQKLVNCPRDVNAHIVGAHGN
pvLDH	LLFEHSGVPKNIIGLGGVLDTSRLKYYISQKLVNCPRDVNAHIVGAHGN
246 250	
hLDHA	SSVPVWSGMNVAGVSLKTLHPDLGTDKKEQWKEVHKQVVEASAYEVIKLLK
pLDH	KMVLKRYITVGGIPLQEFINNK LISDAE LEAIFDRTVNTALEIVNLH
poLDH	KMVLKRYITVGGIPLQEFINNK KITDAE LDAIFDRTVNTALEIVNHY
pmLDH	KMVLKRYITVGGIPLQEFINNK KITDAE LDAIFDRTVNTALEIVNLH
pvLDH	KMVLKRYITVGGIPLQEFINNK KITDEE VEGIFDRTVNTALEIVNLL
246 250	
hLDHA	GYTSAIGLSVADLAESIMKNLRRVHPVSTMIGLYGIKDDVFLSVPCIL
pLDH	ASPYVAPAAAIEMAESYKDLKKVLCSTLLEGQYGHG DIFGGTPLVL
poLDH	ASPYVAPAAAIEMAESYKDLKKVLCSTLLEGQYGHG DIFGGTPLVL
pmLDH	ASPYVAPAAAIEMAESYKDLKKVLCSTLLEGQYGHG DIFGGTPLVL
pvLDH	ASPYVAPAAAIEMAESYKDLKKVLCSTLLEGQYGHG DIFGGTPLVI
hLDHA	GQNGISDLVKVTLTSEEEARLKKSAADTLWGQIKELQF
pLDH	GANGVEQVIELQLNSEEKAKFDEAIAETKRMKALA
poLDH	GCNGVEQVIELQLNSEEKAKFDEAIAETSRMK
pmLDH	GANGVEQVIELQLNSEEKAKFDEAIAETNRMK
pvLDH	GGTGEQVIELQLNSEEKAKFDEAIAETRMK

FIGURE 1: Sequence comparisons of pLDH with human LDH-A (hLDHA). The insertion sequences in the substrate specificity loops are shown in bold, underlined. Residues at the N-terminus corresponding to signature fingerprints of the Rossmann fold are underlined. Important catalytic and cofactor binding residues are in bold.

Table 1: Substrate Kinetic Parameters of pLDH

substrate	k_{cat} (min^{-1})	K_m (μM)	K_{cat}/K_m ($\text{min}^{-1} \text{M}^{-1}$)
pyruvate ^a			
pLDH	$(8.9 \pm 0.3) \times 10^3$	30 ± 3	3.0×10^8
poLDH	$(1.6 \pm 0.03) \times 10^4$	71 ± 4	2.3×10^8
pmLDH	$(7.5 \pm 0.3) \times 10^3$	140 ± 18	5.4×10^7
pvLDH	$(7.6 \pm 0.2) \times 10^3$	17 ± 1	4.4×10^8
lactate ^b			
pLDH	$(3.9 \pm 0.2) \times 10^3$	$12\ 000 \pm 400$	3.3×10^5
poLDH	$(1.5 \pm 0.08) \times 10^3$	$93\ 000 \pm 900$	1.6×10^4
pmLDH	$(2.3 \pm 0.07) \times 10^3$	$11\ 300 \pm 400$	2.0×10^5
pvLDH	$(1.4 \pm 0.03) \times 10^3$	$10\ 200 \pm 700$	1.4×10^5

^a At pH 7.5. ^b At pH 9.2

APAD⁺ (Table 2). Michaelis constants differed up to 4-fold. Of particular interest is the ability of all four pLDH to use APAD⁺ more efficiently than NAD⁺, a property that was used previously to develop an enzyme-based assay for malaria (35, 36). For all four pLDH, the catalytic efficiencies with APAD⁺ are higher than those with NAD⁺, owing to higher k_{cat} values. By comparison, APAD⁺ is a poorer cofactor than NAD⁺ with human LDH (29). It is generally agreed that a conformational change associated with movement of the substrate specificity loop prior to cofactor release is the rate-limiting step in the catalytic cycle of LDH (14). The increased k_{cat} for all pLDH with APAD⁺ suggests that

Table 2: Cofactor Kinetic Parameters of PLDH

cofactor	k_{cat} (min^{-1})	K_{m} (μM)	$K_{\text{cat}}/K_{\text{m}}$ ($\text{min}^{-1} \text{M}^{-1}$)
NADH ^a			
pfLDH	$(8.9 \pm 0.4) \times 10^3$	7 ± 0.8	1.3×10^9
poLDH	$(1.6 \pm 0.03) \times 10^4$	14 ± 0.9	2.3×10^9
pmLDH	$(7.5 \pm 0.2) \times 10^3$	9 ± 0.7	5.4×10^7
pvLDH	$(7.6 \pm 0.2) \times 10^3$	7 ± 1.1	4.4×10^7
NAD ^b			
pfLDH	$(3.9 \pm 0.2) \times 10^3$	86 ± 10	4.5×10^7
poLDH	$(1.5 \pm 0.3) \times 10^3$	311 ± 17	4.8×10^6
pmLDH	$(2.3 \pm 0.05) \times 10^3$	143 ± 11	1.6×10^7
pvLDH	$(1.4 \pm 0.2) \times 10^3$	155 ± 8	9.0×10^6
APAD ^b			
pfLDH	$(1.5 \pm 0.2) \times 10^4$	123 ± 4	1.2×10^8
poLDH	$(9.2 \pm 0.3) \times 10^3$	408 ± 26	2.3×10^7
pmLDH	$(1.4 \pm 0.03) \times 10^4$	168 ± 12	8.0×10^7
pvLDH	$(2.0 \pm 0.04) \times 10^4$	182 ± 13	1.1×10^8

^a At pH 7.5. ^b At pH 9.2.

this conformational change is faster with APAD⁺ bound to the enzyme, compared to NAD⁺, or that another step in the cycle becomes rate-limiting.

Inhibitors of pLDH. Previously, pfLDH was shown to be inhibited by the natural product gossypol and its derivatives and analogues, and the inhibition was competitive with the binding of NADH (20, 29, 37). To test whether the four pLDH were similarly inhibited by these compounds, gossypol and two of its derivatives were examined (Table 3). All four pLDH are inhibited by these compounds; dissociation constants showed a 21-fold range. Dissociation constants were as low as 70 nM. In all cases, inhibition was competitive, as shown in Figure 2.

pH Dependence of Dissociation Constants. The 21-fold range of dissociation constants of inhibitors that bind to the dinucleotide fold (Rossmann fold) of pLDH raised the question of the basis for these differences, especially in view of the similar amino acid composition of the four pLDH in their cofactor binding sites. From comparison of the primary sequences of the pLDH with the crystal structure of pfLDH (14), it appears that pfLDH and pmLDH have identical cofactor binding sites and that poLDH and pvLDH have a single amino acid difference. Nevertheless, there is an 18-fold difference in dissociation constants for the binding of gossypol to pfLDH and pmLDH, despite there being identical residues at the cofactor site. The variation in dissociation constants was not due to pH effects on binding. K_i values for each inhibitor with any of the pLDH were independent of pH in the range pH 6–8.

Substrate Inhibition of pLDH. Substrate inhibition by pyruvate is commonly observed with LDH and has been interpreted as resulting from slow cofactor release that allows time for formation of an NAD⁺–pyruvate adduct during the catalytic cycle (28). pfLDH was unique compared to mammalian LDH in its lack of significant substrate inhibition. The four pLDH were compared with human LDH-A for substrate inhibition, as shown in Figure 3. Neither pmLDH nor poLDH showed substrate inhibition, even at high concentrations of pyruvate. pfLDH and pvLDH showed very little substrate inhibition up to 20 mM pyruvate but modest inhibition at 50 mM pyruvate. By comparison, human LDH-A exhibited inhibition already at low concentrations of pyruvate. Human LDH and many other LDH have a serine

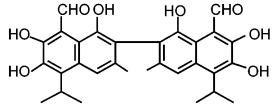
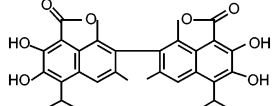
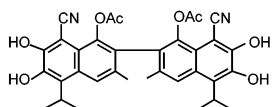
residue at position 163 that interacts with the cofactor. This residue is leucine in all pLDH. Mutation of S163 to L163 in other LDH was shown to remove substrate inhibition (28). The results shown in Figure 5 with pLDH suggest that factors in addition to the residue at position 163 are important contributors to substrate inhibition.

Homology Modeling of pLDH and Molecular Docking. To make a structural comparison at the atomic level, homology models were calculated for *P. vivax*, *P. ovale*, and *P. malariae* using as a template the structure for *P. falciparum* that has been solved to a 1.74 Å resolution (14). As a first step, structures for all three species were generated on the basis of a simultaneous consideration of spatial restraints and local molecular geometry, as implemented in the software Modeler. Modeler considers random backbone deviations of the template protein as a starting point for comparative modeling; however, out of the 100 models generated for each species, the structures exhibiting the lowest root-mean-square deviation from the template invariably resulted in the lowest energy as calculated within the CHARMM force field (38). Because comparison is based on a ternary complex for *P. falciparum* (NADH and the pyruvate analogue oxamic acid), the lowest energy structures from each species, along with the *P. falciparum* template, were subjected to further refinement in the presence of these substrates and explicit solvent. The results are solvated ternary models for each species.

The resulting structures for all four species are strikingly similar and relatively unremarkable. With respect to *P. falciparum*, the backbone root-mean-square deviations for *P. vivax*, *P. ovale*, and *P. malariae* are 0.243, 0.204, and 0.269 Å, respectively (Figure 4). In the same order, the side-chain deviations are 1.56, 1.06, and 1.23 Å. Side-chain substitutions surrounding residues 70–75 and 132–137 in *P. malariae*, 171–177 in *P. ovale*, and 203–207 in *P. vivax* result in small backbone deviations; however, none are in proximity to the active site. Within the active site, little differences are seen aside from subtle changes in the side-chain positioning of R109 and L167 in *P. vivax* and Met 30 in *P. ovale* (Figure 5). Homologous substitutions within the binding pocket (V142A in *P. ovale* and I54V in *P. vivax*) result in little change to the overall binding pocket structures as modeled here, and little deviation can be seen for the β -carbon positioning within both substitutions.

To elucidate binding properties of the gossypol-related inhibitors, docking studies were performed using the four pLDH and gossylic lactone as a representative inhibitor. The dockings were performed in AutoDock 3.0, which allows for conformational flexibility within the inhibitor. As expected from the structural similarities of the models, the binding modes of GL with respect to LDH from all four species were relatively invariant. The studies suggest inhibitor binding within the nicotinamide residue binding area. The finding is consistent with fluorescence quenching data, showing that inhibitor binding was unaffected by the presence of ADP (unpublished data). The tricyclic planes for the inhibitor are in a perpendicular orientation, which is largely necessary to avoid intramolecular steric strain. Out of the two possible perpendicular orientations for the inhibitor, only one is seen in the docking studies. In addition to the hydrophobic interactions with residues involved in nicotinamide residue binding, the 5-isopropyl group shares

Table 3: Dissociation Constants of Inhibitors of pLDH^a

structure	inhibitor	K_i (μ M)			
		pfLDH	pmLDH	pvLDH	poLDH
	gossypol	0.7	12.6	1.4	1.9
	gossylic lactone	0.4	1.5	0.07	0.5
	gossylic nitrile 1,1'-diacetate	0.7	1.8	0.24	0.7

^a All data were obtained at pH 7.5, 25 °C, with pyruvate and NADH as reagents. All inhibitors are competitive with the binding of NADH.

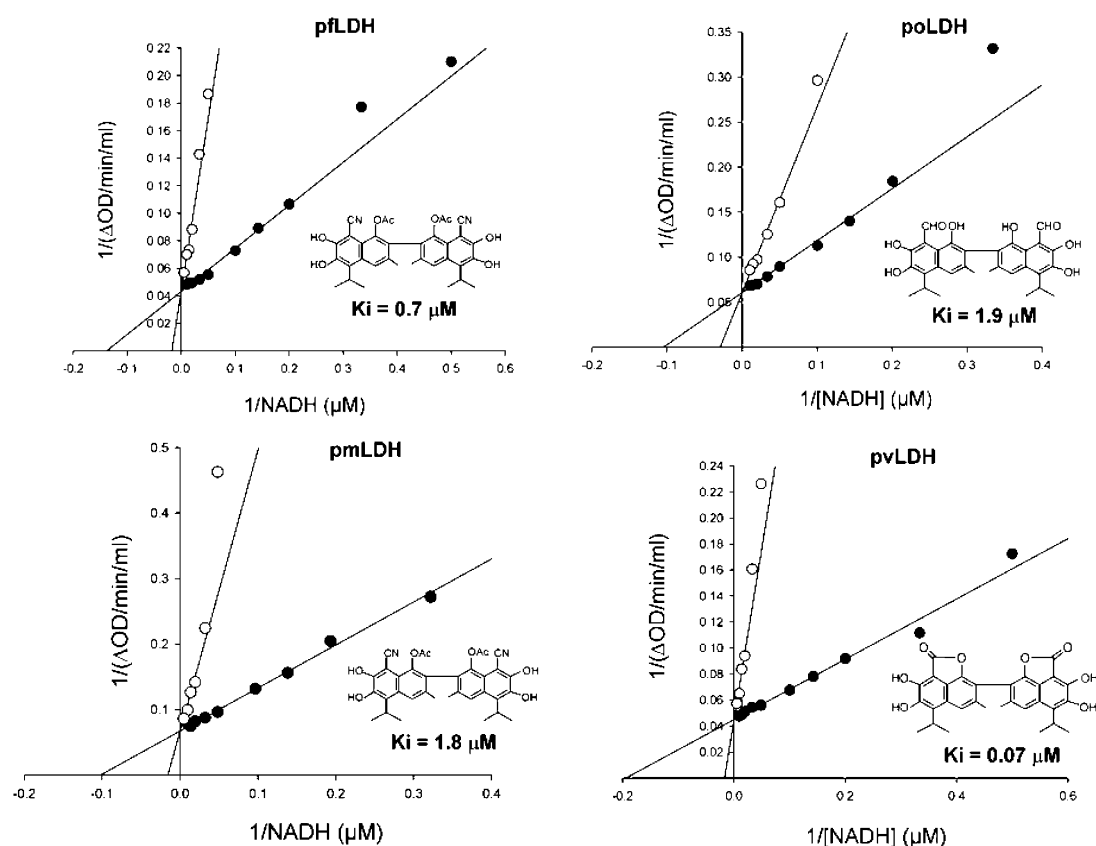


FIGURE 2: Representative patterns of inhibition of pLDH by gossypol and derivatives.

interactions with the pyruvate binding site. The binding energies predicted for the inhibitor for all four species are within the ± 2.177 kcal mol⁻¹ residual standard error reported for the AutoDock empirical free energy function and therefore cannot be used to explain kinetic differences of binding among the species.

DISCUSSION

Apicomplexan LDH. The phylum Apicomplexa includes numerous protozoa, such as species of *Babesia*, *Cryptosporidium*, *Eimeria*, *Theileria*, *Toxoplasma*, and *Plasmodium*, that are responsible for many diseases in humans and animals. Many Apicomplexan parasites, including *Plasmo-*

dium, depend heavily upon anaerobic glycolysis for energy production, suggesting that glycolytic enzymes, including LDH, represent potential drug targets. This present study compared pLDH from the four species of human malarial parasite in terms of structure and kinetic properties. pLDH from all four species of *Plasmodium* exhibit the same five-amino-acid insert in their substrate specificity loops (Figure 1). This feature of pLDH, which is unusual compared with other LDH, was first noted for pfLDH (13). Crystallography studies of pfLDH demonstrated that this insert provided a unique active-site architecture that might be exploited for drug development (14). Subsequently, *T. gondii* was shown to express different LDH in the tachyzoite and bradyzoite stages of development, both of which also have five-amino-

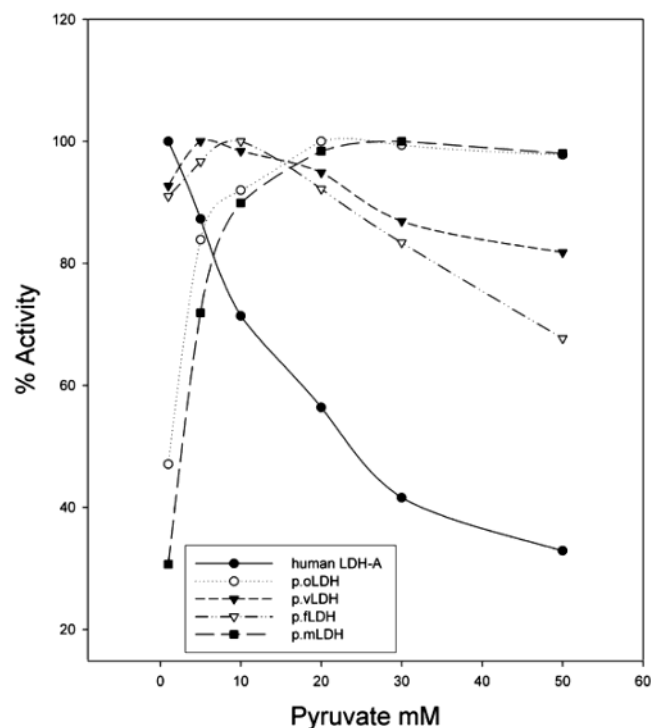


FIGURE 3: Substrate inhibition patterns of pLDH compared to human LDH-A.

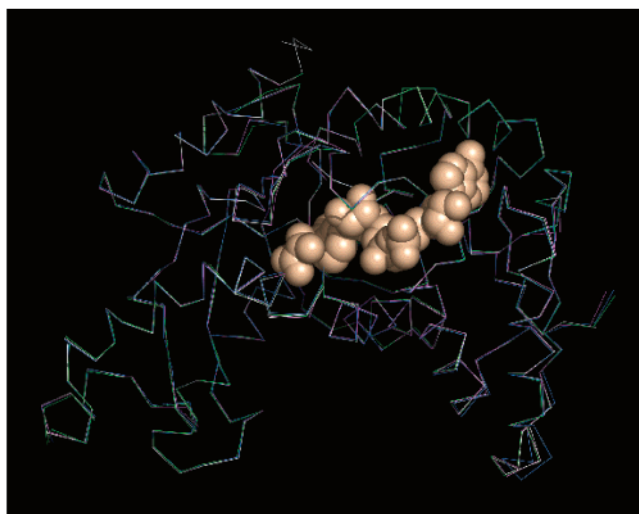


FIGURE 4: Backbone trace of pLDH from *P. falciparum* (white), *P. vivax* (magenta), *P. ovale* (green), and *P. malariae* (blue), with NADH and oxamic acid ligands shown in a CPK representation.

acid inserts in their substrate specificity loops (25, 26). In view of the many biochemical similarities between *T. gondii* and *P. falciparum* (22, 23), it was anticipated that pvLDH, poLDH, and pmLDH from the other species of *falciparum* would not differ markedly from pfLDH with respect to their substrate specificity loops and that all pLDH would have five-amino-acid inserts. This structural feature of an extended specificity loop from the five-amino-acid insert, however, is not observed with all Apicomplexan LDH. Recently the sequence of LDH from *Cryptosporidium parvum* was reported (39). This LDH, designated CpLDH1, does not have the five-amino-acid insert in the substrate specificity loop, although sequence alignment suggests that the aspartate residue corresponding to the first residue in the insert may be present. Thus, *Plasmodium* species and *T. gondii* are the

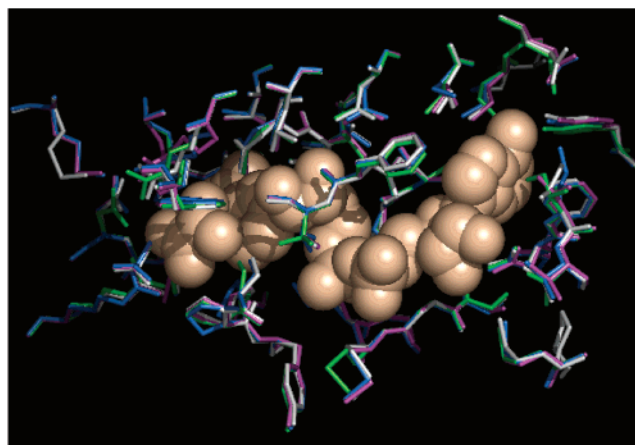


FIGURE 5: Ligand binding pockets from pfLDH (white), pvLDH (magenta), poLDH (green), and pmLDH (blue), with NADH and oxamic acid ligands shown in a CPK representation.

only presently known sources of LDH with extended substrate specificity loops.

Apicomplexan LDH as Drug Targets. The shrinking drug arsenal of effective therapeutics for treating infections by *P. falciparum* likely will extend to other *Plasmodium* infections as drug resistance spreads. For infections by other Apicomplexan parasites, the situation is equally serious. For example, there are very few effective drugs for treatment of toxoplasmosis or cryptosporidiosis. Any glycolytic enzyme is a potential target for development of new drugs, especially those with unique features compared with their human counterpart. On this basis, the unique active-site architecture of pLDH is especially attractive. However, glycolytic enzymes in malarial parasites present special problems as potential drug targets. These enzymes are present at quite high concentrations (3). For example, we estimate that the trophozoite stage of *P. falciparum* has 3–5 μM concentrations of pfLDH. This is based upon studies of the volumes of purified parasites and measurement of the specific activity of pfLDH in lysed parasites compared with the specific activity of the purified enzyme. This high concentration of pLDH suggests that high concentrations of inhibitors as potential antimalarials will be required, unless very high affinity inhibitors are developed. For example, a 1 nM steady-state concentration of inhibitor is sufficient to produce 90% inhibition of 5 μM pLDH if the dissociation constant is 10^{-10} M.

Substrate Specificity of pLDH. The four pLDH share the same catalytic residues that are conserved in all LDH, including R109, D168, H195, and R171 (Figure 1). The mechanism of all LDH includes ternary complex formation by ordered addition of NADH and pyruvate, followed by a rate-determining conformational change in which a substrate specificity loop closes to form a desolvated ternary complex. This brings R109 into the active site to polarize the ketone carbonyl of pyruvate. Hydride is transferred rapidly from NADH to the polarized ketone group, facilitated by proton donation from the D168/H195 couple. R171 anchors pyruvate by interaction with the carboxylate functional group (14). Residues 98–109 (standard numbering for LDH) in most LDH form a mobile loop that closes in the ternary complex to form the catalytic site. In pLDH and in LDH1 and LDH2 from *T. gondii*, the five-amino-acid insert and other amino acid differences in the rest of the loop raise the

question whether the substrate specificities of pLDH, LDH1, and LDH2 differ from those of other LDH. For example, conserved Q102 in many LDH resides in a pocket into which the methyl group of pyruvate inserts. Conversion of Q102 into R102 in LDH from *Bacillus stearothermophilus*, which provide the positively charged R102 as a counterion to bind the side chain of oxaloacetate, converts this LDH into a malate dehydrogenase (40). All pLDH as well as LDH1 and LDH2 have lysine at position 102. These LDH might be expected to exhibit malate dehydrogenase activity; however, there is no detectable malate dehydrogenase activity. Likewise, the extended loop might be expected to expand the substrate specificity of pLDH, LDH1, and LDH2. Addition of a longer specificity loop into LDH from *B. stearothermophilus* leads to a loss of activity with pyruvate but retention of activity with phenylpyruvate, thereby turning this LDH into a phenyllactate dehydrogenase (41). Both LDH1 and LDH2 can utilize phenylpyruvate (27). By comparison, none of the pLDH utilize this substrate. Thus, all four pLDH retain a high selectivity for pyruvate, despite their extended specificity loops.

pLDH Compared to Parasite Malate Dehydrogenases. The lack of malate dehydrogenase (MDH) activity of the four pLDH, despite the presence of a positively charged residue at position 102, is especially interesting in light of recent evolutionary studies of LDH and MDH (39, 42). MDH is found in all life domains, whereas LDH is limited to bacteria and eukarya. Phylogenetic studies suggest that two ancestral gene duplications resulted in three major clades: the first includes the two subgroups of dimeric MDH found in cytosol and mitochondria; the second includes the recently recognized tetrameric LDH-like MDH; and the third includes the tetrameric LDH (42). It has been proposed that the LDH resulted from an ancient duplication of LDH-like MDH. However, Apicomplexan LDH are monophyletic to α -proteobacterial LDH-like MDH, suggesting that Apicomplexan LDH were acquired, either by lateral gene transfer or by the endosymbiosis that produced mitochondria, from an LDH-like MDH (39, 42). In this scenario, Apicomplexan LDH evolved from an ancestral LDH-like MDH after Apicomplexa diverged from other eukaryotes. The significance of this is that Apicomplexan LDH resemble LDH-like MDH more than they resemble other LDH. This may have important implications in the development of selective inhibitors of pLDH.

Most MDH, including LDH-like MDH, have an arginine residue at position 102 in the substrate binding site, whereas most LDH have glutamine at this position. All Apicomplexan LDH examined thus far have lysine at position 102, except CpLDH1 from *T. gondii*, which has a glycine residue at position 102. This is readily accounted for by single base mutations; four of the six codons for arginine can be converted into the four codons for glycine by a C-to-G change in the first base; the remaining two arginine codons can be converted into the two codons for lysine by conversion of G to A in the second base. Less easy to explain, however, is the lack of MDH activity in the Apicomplexan LDH that have lysine at position 102.

Cofactor Selectivity of pLDH. The previously observed ability of pLDH, LDH1, and LDH2 to utilize APAD⁺ as cofactor efficiently extends to poLDH, pvLDH, and pmLDH (Table 2). All four pLDH utilize APAD⁺ more efficiently

than NAD⁺, which was also observed with LDH1 and LDH2 (27). By comparison, other LDH utilize APAD⁺ much less efficiently. This ability to use APAD⁺ as cofactor may be a common property of Apicomplexan LDH. CpLDH1 from *C. parvum* also can utilize APAD⁺ (Vander Jagt and Zhu, unpublished results). In all cases with parasite LDH, the increased efficiency, k_{cat}/K_m , is the result of enhanced k_{cat} values. In some cases, K_m is lower, which also contributes to the increased efficiency (27). Since loop movement is thought to be rate-determining for LDH, this suggests that loop movement for all four pLDH as well as for LDH1 and LDH2 is faster when APAD⁺ replaces NAD⁺. Alternatively, another step in the catalytic cycle becomes rate-limiting when APAD⁺ replaces NAD⁺. This would still require that loop movement be faster when APAD⁺ replaces NAD⁺ as substrate.

A recent crystallography and kinetic study of LDH1 provides additional insight into the mechanism of Apicomplexan LDH and an explanation for the enhanced activity with APAD⁺ (43). Comparison of the crystal structures of the LDH1–NAD⁺–oxalate and LDH1–APAD⁺–oxalate ternary complexes demonstrated essentially identical side-chain conformations of active-site residues. In addition, temperature factors of main-chain atoms in the two structures were similar, suggesting that energetics of binding of APAD⁺ to LDH1 is not fundamentally different from the binding of NAD⁺. This would question whether the rate of loop movement is markedly different when APAD⁺ replaces NAD⁺. However, since APAD⁺ has a higher oxidation potential than NAD⁺, hydride transfer to APAD⁺ would be expected to be faster than transfer to NAD⁺, and this could explain the kinetic differences between the two cofactors if chemistry steps are at least partly rate-limiting. This was supported by the observation that the LDH1-catalyzed oxidation of lactate is faster with APAD⁺ than with NAD⁺, but the reduction of pyruvate is faster with NADH than with APADH, which is as predicted if hydride transfer were partially rate-limiting.

Substrate Inhibition. Substrate inhibition is a common property of LDH. The mechanism of substrate inhibition involves the formation at the active site of a covalent complex between pyruvate and NAD⁺ (18). Conserved S163 has been considered to be a critical residue that contributes to substrate inhibition in other LDH (28, 44). Crystallography data of LDH indicate that the hydroxyl group of S163 interacts through a bridging water molecule with the amide of the nicotinamide moiety in NADH. This affects the rate of release of NAD⁺ after the reduction of pyruvate and release of lactate. The residence time of NAD⁺ determines whether pyruvate can bind, after which an adduct can form, presumably by addition of the C4 carbon of the nicotinamide ring to the enol form of pyruvate. Mutation of S163 has pronounced effects on substrate inhibition. The S163A mutant of human LDH-A retains substrate inhibition, while the S163L mutant has lost substrate inhibition (28, 44). It is not clear whether the water molecule is retained in the S163A mutant. It appears to be absent in the S163L mutant due to steric limitations, on the basis of modeling studies (45). In all four pLDH, S163 is replaced by L163 (Figure 1). At first glance, this would appear to explain the lack of substrate inhibition or the diminished level of substrate inhibition observed with the four pLDH compared to human LDH-A

(Figure 3). However, the explanation must be more complicated. The S163L mutant of LDH-A exhibits a 40-fold increase in the K_m for pyruvate compared to the native enzyme. Thus, loss of substrate inhibition in this mutant appears to be the result of weaker binding of pyruvate to the enzyme–NAD⁺ complex rather than altered residence time of NAD⁺. This is supported by the observation that the dissociation constant of the pyruvate analogue oxamate in the S163L mutant LDH–NADH–oxamate ternary complex is increased 120-fold compared to the wild-type, whereas the dissociation constant for NAD⁺, determined by fluorescence titration, is essentially unchanged from that for the native enzyme. By comparison, all four pLDH show Michaelis constants for pyruvate (Table 1) that are comparable to that of native human LDH-A (34). Therefore, the S163L mutant of LDH-A does not appear to be a good model of pLDH, and explanations for the weak or absent substrate inhibition in pLDH are more complicated than the nature of the residue at position 163. This LDH-A model also is insufficient to explain the results with LDH1 and LDH2 from *T. gondii*. Both of these LDH have methionine residues at position 163, unlike either pLDH or most other LDH. However, substrate inhibition is observed with LDH1 but not with LDH2.

Inhibitors of pLDH. Inhibition of all four pLDH by gossypol and derivatives (Table 3) is strictly competitive with cofactor binding (Figure 2). This is consistent with previous studies of human LDH and pfLDH for inhibition by these types of compounds (19, 20, 29, 34). Although it is not generally thought that the cofactor binding site might be a target for drug development, this suggestion deserves evaluation. Similar arguments were made concerning development of selective protein kinase inhibitors that bind to the ATP binding site, which is structurally similar in many protein kinases. Nevertheless, highly selective protein kinase inhibitors are now being evaluated clinically (46).

The idea of Apicomplexan LDH as potential drug targets raises the question whether selective inhibition of parasite LDH compared to human LDH is a realistic goal. The crystal structures of pfLDH and LDH1 (14, 43) as well as a recent crystal structure of pLDH from *Plasmodium berghei* (47) demonstrate significant structural differences, such as the extended specificity loop, that might be exploited in drug design. In addition, the cofactor binding sites exhibit differences compared to human LDH that might be exploited. A related question is whether selective inhibitors of Apicomplexan LDH can be developed that do not inhibit human MDH, in view of the fact that Apicomplexan LDH appear to have evolved from an LDH-like MDH (39, 42). Thus, drug development will need to consider both human LDH and MDH in the quest for selective inhibitors of Apicomplexan LDH.

The dissociation constants for inhibition of pLDH (Table 3) show a 21-fold range that is not predictable from comparisons of the cofactor binding sites. For example, pfLDH and pmLDH appear to have almost identical cofactor binding sites with no amino acid differences among residues that interact with the cofactor, yet there is an 18-fold difference in the dissociation constants for gossypol (0.7 and 12.6 μ M for pfLDH vs pmLDH) but less than a 3-fold difference for pvLDH and poLDH compared to pfLDH (1.4 and 1.9 μ M for pvLDH and poLDH), even though both

pvLDH and poLDH have one residue difference than pfLDH at the cofactor site; pvLDH has V54 rather than I54 and poLDH has A142 rather than V142. And although there is an 18-fold difference in the dissociation constants of pfLDH and pmLDH for gossypol, there is less than a 3-fold difference for gossylic nitrile 1,1'-diacetate. Likewise, the dissociation constants for gossypol in comparing pfLDH vs pvLDH suggest higher affinity for pfLDH, whereas the reverse is true when comparing these two pLDH with gossylic lactone and gossylic nitrile 1,1'-diacetate. The lack of a pH effect on binding between pH 6 and 8 suggests that neither the ionization state of residues at the cofactor site that may participate in binding of the inhibitors nor the ionization state of the inhibitors is pH-dependent in this pH range. Previous studies of human LDH-A and LDH-B (also called LDH-M and LDH-H), in which the kinetic properties were compared with the crystal structures in an attempt to explain the different activities of these two LDH, demonstrated that the structures are nearly identical at the active sites (48). Nevertheless, the kinetic properties, especially the Michaelis constants for pyruvate, are different and are pH-dependent. This was ascribed to altered pK_a values of the catalytic residue H195 between the two isozymes as a result of electrostatic perturbations produced by surface residues. Cofactor binding, however, was similar between the two isozymes, suggesting that surface electrostatics did not influence cofactor binding. Thus, the different apparent isoelectric points for the four pLDH, which suggests different surface charges, do not appear to account for variations in the binding of inhibitors to the cofactor site. Differences that are not apparent produce the 21-fold range of dissociation constants, corresponding to about 1.8 kcal mol⁻¹ differences in binding energies.

Computational Studies. The kinetic differences seen upon inhibition by the gossypol-related compounds for the four species are too small to rely on an explanation based on the docking methods presented herein. Additionally, the structural similarities found for the models of pLDH preclude any explanation of these differences based on a static interpretation of the protein. However, the following significant findings with respect to pLDH as a drug target for malaria are noted: the structures of LDH among all four species are predicted to be strikingly similar, the binding modes of gossylic lactone are relatively invariant, and therefore drugs targeted to pLDH from one species are expected to be efficacious against all four. Out of the two perpendicular orientations expected for the tricyclic planes of the inhibitor, only one is seen in docking studies, suggesting that atropoisomerism about the binaphthyl bond will impact the kinetics of racemic mixtures of the inhibitor. Finally, the inhibitor is predicted to bind in the nicotamide residue binding region of the active site. In this orientation, the inhibitor shares interactions with a substrate-binding residue. Therefore, inhibitor binding affinity and selectivity for the enzyme over other oxidoreductases that utilize NADH can likely be improved via appropriate ring substitution such that the inhibitors utilize active-site interactions with both cofactor and substrate binding residues.

REFERENCES

1. Krogstad, D. J. (1996). Malaria as a reemerging disease, *Epidemiol. Rev.* 18, 77–89.

2. Barat, L. M., and Bloland, P. B. (1997). Drug resistance among malaria and other parasites, *Infect. Dis. Clin. North Am.* 11, 969–987.
3. Vander Jagt, D. L., Hunsaker, L. A., Campos, N. M., and Baack, B. R. (1990) D-Lactate formation in human erythrocytes infected with *Plasmodium falciparum*, *Mol. Biochem. Parasitol.* 42, 277–284.
4. Scheibel, L. W., and Pflaum, W. K. (1970) Carbohydrate metabolism in *Plasmodium knowlesi*, *Comp. Biochem. Physiol.* 37, 543–553.
5. Sherman, I. W. (1979) Biochemistry of *Plasmodium* (malaria parasites), *Microbiol. Rev.* 43, 453–495.
6. Certa, U., Ghersa, P., Dobeli, H., Matile, H., Kocher, H. P., Shrivastava, I. K., Shaw, A. R., and Perin, L. H. (1988). Aldolase Activity in a *Plasmodium falciparum* protein with protective properties, *Science* 240, 1036–1038.
7. Kaslow, D. C., and Hill, S. (1990). Cloning metabolic pathway genes by complementation in *Escherichia coli*: Isolation and expression of *Plasmodium falciparum* glucose phosphate isomerase, *J. Biol. Chem.* 265, 12337–12341.
8. Hicks, E., Read, M., Holloway, S. P., Sims, P. F. G., and Hyde, J. E. (1991). Glycolytic pathway of the human malaria parasite *Plasmodium falciparum*: Primary sequence analysis of the gene encoding 3-phosphoglycerate kinase and chromosomal mapping studies, *Gene* 100, 123–129.
9. Olafsson, P., Matile, H., and Certa, U. (1992). Molecular analysis of *Plasmodium falciparum* hexokinase, *Mol. Biochem. Parasitol.* 56, 89–102.
10. Daubenberger, C. A., Polt-Frank, F., Jiang, G., Lipp, J., Certa, U., and Pluschke, G. (2002) Identification and recombinant expression of glyceraldehydes-3-phosphate dehydrogenase of *Plasmodium falciparum*, *Gene* 246, 255–264.
11. Read, M., Hicks, K. E., Sims, P. F. G., and Hyde, J. E. (1994). Molecular characterisation of the enolase gene from the malaria parasite *Plasmodium falciparum*. Evidence for ancestry within a photosynthetic lineage, *Eur. J. Biochem.* 220, 513–520.
12. Ranie, J., Kumar, V. P. H., and Balaram, H. (1993). Cloning of the triose-phosphate isomerase gene of *Plasmodium falciparum* and expression in *Escherichia coli*, *Mol. Biochem. Parasitol.* 61, 159–169.
13. Bzik, D. J., Fox, B. A., and Gonyer, K. (1993). Expression of *Plasmodium falciparum* lactate dehydrogenase in *Escherichia coli*, *Mol. Biochem. Parasitol.* 59, 155–166.
14. Dunn, C. R., Banfield, M. J., Barker, J. J., Higham, C. W., Moreton, K. M., Brady, R. L., and Holbrook, J. J. (1996) The structure of lactate dehydrogenase from *Plasmodium falciparum* reveals a new target for anti-malarial design, *Nat. Struct. Biol.* 3, 912–915.
15. Velanker, S. S., Ray, S. S., Gokhale, R. S., Suma, S., Balaram, H., Balaram, P., and Murthy, M. R. (1997). Triosephosphate isomerase from *Plasmodium falciparum*: the crystal structure provides insights into antimalarial drug design, *Structure* 5, 751–761.
16. Kim, H., Certa, U., Dobeli, H., Jakob, P., and Hol, W. G. (1998). Crystal structure of fructose-1,6-bisphosphate aldolase from the human malaria parasite *Plasmodium falciparum*, *Biochemistry* 31, 4388–4396.
17. Vander Jagt, D. L., Hunsaker, L. A., and Heidrich, J. E. (1981). Partial purification and characterization of lactate dehydrogenase from *Plasmodium falciparum*, *Mol. Biochem. Parasitol.* 4, 255–264.
18. Dunn, C. R., Wilks, H. M., Halsall, D. J., Atkinson, T., Clarke, A. R., Muirhead, H., and Holbrook, J. J. (1991). Design and synthesis of new enzymes based on the lactate dehydrogenase framework, *Philos. Trans. R. Soc. London B* 332, 177–184.
19. Royer, R. E., Deck, L. M., Campos, N. M., Hunsaker, L. A., and Vander Jagt, D. L. (1986). Biologically active derivatives of gossypol: Synthesis and antimalarial activities of peri-acylated gossypol nitriles, *J. Med. Chem.* 29, 1799–1801.
20. Deck, L. M., Royer, R. E., Chamblee, B. B., Hernandez, V. M., Malone, R. R., Torres, J. E., Hunsaker, L. A., Piper, R. C., Makler, M. T., and Vander Jagt, D. L. (1998). Selective inhibitors of human lactate dehydrogenases and lactate dehydrogenase from the malarial parasite *Plasmodium falciparum*, *J. Med. Chem.* 41, 3879–3887.
21. Remington, J. S., and Desmonts, G. Toxoplasmosis. In *Infectious Diseases of the Fetus and Newborn Infant* (Remington, J. S., and Klein, J. O., Eds.) pp 89–195, WB Saunders and Co., Philadelphia, 1990.
22. Roos, D. S., Crawford, M. J., Donald, R. G., Fohl, L. M., Hager, K. M., Kissinger, J. C., Reynolds, M. G., Striepen, B., and Sullivan, W. J., Jr. (1999). Transport and trafficking: *Toxoplasma* as a model for *Plasmodium*, *Novartis Found. Symp.* 226, 176–195.
23. Waller, R. F., Keeling, P. J., Donald, R. G., Striepen, B., Handman, E., Lang-Unnasch, N., Cowman, A. F., Besra, G. S., Roos, D. S., and McFadden, G. I. (1998) Nuclear-encoded proteins target to the plastid in *Toxoplasma gondii* and *Plasmodium falciparum*, *Proc. Natl. Acad. Sci.* 95, 12352–12357.
24. Dzierszinski, F., Popescu, O., Toursel, C., Slomianny, C., Yahiaoui, B., and Tomavo, S. (1999). The protozoan parasite *Toxoplasma gondii* expresses two functional plant-like glycolytic enzymes. Implications for evolutionary origin of apicomplexans, *J. Biol. Chem.* 274, 24888–24895.
25. Yang, S., and Parmley, S. F. (1995). A bradyzoite stage-specifically expressed gene of *Toxoplasma gondii* encodes a polypeptide homologous to lactate dehydrogenase, *Mol. Biochem. Parasitol.* 73, 291–294.
26. Yang, S., and Parmley, S. F. (1997). *Toxoplasma gondii* expresses two distinct lactate dehydrogenase homologous genes during its lifecycle in intermediate hosts, *Gene* 184, 1–12.
27. Dando, C., Schroeder, E. R., Hunsaker, L. A., Deck, L. M., Royer, R. E., Zhou, X., Parmley, S. F., and Vander Jagt, D. L. (2001). The kinetic properties and sensitivities to inhibitors of lactate dehydrogenases (LDH-1 and LDH-2) from *Toxoplasma gondii*: Comparison with pLDH from *Plasmodium falciparum*, *Mol. Biochem. Parasitol.* 118, 23–32.
28. Hewitt, C. O., Eszes, C. M., Sessions, R. B., Moreton, K. M., Dafforn, T. R., Takei, J., Dempsey, C. E., Clarke, A. R., and Holbrook, J. J. (1999). A general method for relieving substrate inhibition in lactate dehydrogenases, *Protein Eng.* 12, 491–496.
29. Gomez, M. S., Piper, R. C., Hunsaker, L. A., Royer, R. E., Deck, L. M., Makler, M., and Vander Jagt, D. L. (1997) Substrate and cofactor specificity and selective inhibition of lactate dehydrogenase from the malarial parasite *P. falciparum*, *Mol. Biochem. Parasitol.* 90, 235–246.
30. Sali, A., and Blundell, T. (1993). Comparative protein modeling by satisfaction of spatial restraints, *J. Mol. Biol.* 234, 779–815.
31. McLachlan, A. D. (1982). Rapid comparison of protein structures, *Acta Crystallogr. Sect. A—Found. Crystallogr.* 38, 871–873.
32. Laskowski, R. A., MacArthur, M. W., Moss, D. S., and Thornton, J. M. (1993). PROCHECK: a program to check the stereochemical quality of protein structures, *J. Appl. Crystallogr.* 26, 283–291.
33. Morris, G. M., Goodsell, D. S., Halliday, R. S., Huey, R., Hart, W. E., Belew, R. K., and Olson, A. J. (1998) Automated docking using a Lamarckian genetic algorithm and empirical binding free energy function, *J. Comput. Chem.* 19, 1639–1662.
34. Yu, Y., Deck, J. A., Hunsaker, L. A., Deck, L. M., Royer, R. E., Goldberg, E., and Vander Jagt, D. L. (2001) Selective active site inhibitors of human lactate dehydrogenases A4, B4, and C4, *Biochem. Pharmacol.* 61, 81–89.
35. Makler, M. T., Ries, J. A., Williams, J. E., Bancroft, R. C., Piper, B. L., Gibbins, B. L., and Hinrichs, D. J. (1993) Parasite lactate dehydrogenase as an assay for *Plasmodium falciparum* drug sensitivity, *Am. J. Trop. Med. Hyg.* 48, 739–741.
36. Makler, M. T., and Hinrichs, D. J. (1993) Measurement of the lactate dehydrogenase activity of *Plasmodium falciparum* as an assessment of parasitemia, *Am. J. Trop. Med. Hyg.* 48, 205–210.
37. Vander Jagt, D. L., Deck, L. M., and Royer, R. E. (2000) Gossypol: prototype of inhibitors targeted to dinucleotide folds, *Curr. Med. Chem.* 7, 479–498.
38. Brooks, B., Bruccoleri, R., Olafson, B., States, D., Swaminathan, S., and Karplus, M. (1983) CHARMM—a program for macromolecular energy, minimization, and dynamics calculations, *J. Comput. Chem.* 4, 187–217.
39. Zhu, G., and Keithly, J. S. (2002) α -Proteobacterial relationships of apicomplexan lactate and malate dehydrogenases, *J. Eukaryot. Microbiol.* 49, 255–261.
40. Wilks, H. M., Hart, K. W., Feeney, R., Dunn, C. R., Muirhead, H., Chia, W. N., Barstow, D. A., Atkinson, T., Clarke, A. R., and Holbrook, J. J. (1988) A specific, highly active malate dehydrogenase by redesign of the lactate dehydrogenase framework, *Science* 242, 1541–1544.
41. Wilks, H. M., Moreton, K. M., Halsall, D. J., Hart, K. W., Sessions, R. D., Clarke, A. R., and Holbrook, J. J. (1992) Design of a specific phenyllactate dehydrogenase by peptide loop exchange on the *Bacillus stearothermophilus* lactate dehydrogenase framework, *Biochemistry* 31, 7802–7806.

42. Madern, D. (2002) Molecular evolution within the L-malate and L-lactate dehydrogenase superfamily, *J. Mol. Evol.* 54, 825–840.
43. Kavanagh, K. L., Elling, R. A., and Wilson, D. K. (2004) Structure of *Toxoplasma gondii* LDH1: Active-site differences from human lactate dehydrogenases and the structural basis for efficient APAD⁺ use, *Biochemistry* 43, 879–889.
44. Eszes, C. M., Sessions, R. B., Clark, A. R., Moreton, K. M., and Holbrook, J. J. (1996) Removal of substrate inhibition in a lactate dehydrogenase from human muscle by a single residue change, *FEBS Lett.* 399, 193–197.
45. Wigley, D. B., Gamblin, S. J., Turkenburg, J. P., Dodson, E. J., Piontek, K., Muirhead, H., and Holbrook, J. J. (1992) Structure of a ternary complex of an allosteric lactate dehydrogenase from *Bacillus stearothermophilus* at 2.5 Å resolution, *J. Mol. Biol.* 223, 317–335.
46. Parasrampur, D. A., de Boer, P., Desai-Krieger, D., Chow, A. T., and Jones, C. R. (2003) Single-dose pharmacokinetics and pharmacodynamics of RWJ 67657, a specific p38 mitogen-activated protein kinase inhibitor: a first-in-human study, *J. Clin. Pharmacol.* 43, 406–413.
47. Winter, V. J., Cameron, A., Tranter, R., Sessions, R. B., and Brady, R. L. (2003) Crystal structure of *Plasmodium berghei* lactate dehydrogenase indicates the unique structural differences of these enzymes are shared across the *Plasmodium* genus, *Mol. Biochem. Parasitol.* 131, 1–10.
48. Read, J. A., Winter, V. J., Eszes, C. M., Sessions, R. B., and Brady, R. L. (2001) Structural basis for altered activity of M- and H-isozyme forms of human lactate dehydrogenase, *Proteins* 43, 175–185.

BI049892W